

Uyen Thi Phan Ngoc and Dai Hai Nguyen*

Synergistic antifungal effect of fungicide and chitosan-silver nanoparticles on *Neoscytalidium dimidiatum*

DOI 10.1515/gps-2016-0206

Received November 23, 2016; accepted March 9, 2017; previously published online May 19, 2017

Abstract: Chitosan-silver nanoparticles (Ag@CS) as a novel drug delivery system have been developed for fungicide drug. In this study, the synergistic effect of silver nanoparticles (AgNPs), chitosan (CS), and fungicide zineb (Zi) was investigated as antifungal materials against *Neoscytalidium dimidiatum* in dragon fruit. More specifically, Ag@CS were prepared by embedding of AgNPs in CS polymer and then combined with Zi. Transmission electron microscopy was used to confirm the morphology and size of Ag@CS. The diameter of spherical nanoparticles is around 4.11 ± 0.37 nm. Furthermore, the formation of Ag@CS was characterized by Fourier transform infrared and X-ray diffraction analysis. The thermostability properties of these nanoparticles were also determined by thermogravimetric analysis. Especially the antifungal activity of Ag@CS has shown antifungal ability better than each component alone, analyzed by zone of inhibition method against *N. dimidiatum*. These results suggest the potential applications of Ag@CS in the development of nanomaterials for antibiotic application.

Keywords: antifungal activity; chitosan; fungicide; *Neoscytalidium dimidiatum*; silver nanoparticle.

1 Introduction

Dragon fruit or pitahaya (*Hylocereus undatus*) is commonly known as a nutritious fruit, has become a main crop with large acreage, and is a high-income earner. It is considered

as a good source of potassium, phosphorus, vitamin C (ascorbic acid), calcium, carbohydrates, and fiber, which can reduce the risk of stroke and coronary heart disease by preventing high cholesterol and improving the digestive system with its fiber and also avoiding cancer. Up to now, Vietnam is one country that provides dragon fruit on commercial scale for China, Hong Kong, Japan, Singapore, and many countries in Europe. According to data from the Department of Crop Production and the Ministry of Agriculture and Rural Development, the area planted with dragon fruit reached more than 28,700 ha with production of 520,000 tons/year that occupied 61.4% for totally fresh fruit export [1, 2]. However, when growing dragon fruit in a large area, farmers have to face a lot of difficulties in preventing diseases caused by microorganisms. *Neoscytalidium dimidiatum*, the pathogen of pitahaya brown spot disease, is one of the most dangerous plant pathogens that cause great losses in agricultural crops, especially in dragon fruit. It affects not only the export fruit productivity but also the economic outcomes. To prevent brown rot disease, chemical drugs were used commonly in agriculture due to their effective disease treatment [3–5]. However, incorrect use of drug or inefficient dosage may prolong treatment time and reduce crop yields. In addition, low-quality chemicals can lead to disastrous consequences, resulting in increasing the manufacturing costs, low control, low productivity, and low profits [6, 7]. Furthermore, disease outbreak means that farmers often use high doses of antibiotics leading to drug amounts exceeding the permitted level, which could destroy beneficial insects in the soil and create pathogen resistance [8–11]. As a consequence, reduced productivity, quality of crops, and negative impacts on the environment and human health occur [6, 12, 13].

Recently, silver nanoparticles (AgNPs) have been combined with different kinds of nanofibers and drugs to increase antimicrobial efficacy for antimicrobial applications. Since the early twentieth century, Ag has been used as one of the typical ingredients in alternative medicine and functional food [14–18]. It also has been used in the photo industry since the 1800s, sterilization of drinking water, and in disinfection of swimming pools [19, 20]. Moreover, Kokura [21] reported that AgNPs at low concentration had sufficient preservation efficacy against bacteria

*Corresponding author: Dai Hai Nguyen, Institute of Applied Materials Science, Vietnam Academy of Science and Technology, 01 TL29, District 12, Ho Chi Minh City 700000, Vietnam; and Graduate University of Science and Technology, Vietnam Academy of Science and Technology, Hanoi, Vietnam, e-mail: nguyendaihai0511@gmail.com

Uyen Thi Phan Ngoc: Institute of Applied Materials Science, Vietnam Academy of Science and Technology, 01 TL29, District 12, Ho Chi Minh City 700000, Vietnam; and Graduate University of Science and Technology, Vietnam Academy of Science and Technology, Hanoi, Vietnam

and fungi and did not penetrate normal human skin in cosmetic application. Importantly, the antimicrobial activities of AgNPs were also studied successfully in Kyung-Hwan Cho's research at 5–10 ppm [22] and at 20 ppm in Sotiriou's study [23]. A number of independent cytotoxicity tests have been completed on American Biotech Lab AgNPs products. At 10–22 ppm, no damages were found when the AgNPs products were tested with either human or monkey cells, which means that they were completely non-cytotoxic [24–26]. In addition, chitosan (CS), an abundant natural hydrophilic biopolymer, has been commonly chosen to combine with AgNPs due to their unlimited biocompatibility, biodegradability, better stability, and low toxicity [8, 27–30]. Many studies showed that this polymer acts as plant growth stimulant that helps the plant resist infection from microbes activity [8, 31–33], has good antibacterial properties [8, 34–36], and stimulates immunity of the plant system [37, 38]. With these advantages, the combination of CS and AgNPs (Ag@CS) is a potential approach for antimicrobial targets. As an expected result, the bio-nanocomposite exhibits higher antibacterial activity than any component acting alone. This system deserves attention as one of the expanded applications of Ag@CS that can act as a safe fungicide for nanotechnology and agriculture.

In this research, zineb (Zi) combined with Ag@CS (Ag@CS-Zi) against *N. dimidiatum* was developed. The synthesis of AgNPs enveloped in the biopolymer CS was studied for production of bio-nanocomposites with enhanced antifungal properties. The study focused on Ag@CS synthesis and testing their fungicidal properties. In addition, the nanoparticles were characterized by Fourier transform infrared (FT-IR), X-ray diffraction (XRD), transmission electron microscopy (TEM), and thermal-gravimetric analysis (TGA). Furthermore, the antifungal activities of the composite against fungi were examined using inhibition zone method on potato dextrose agar (PDA) plate. The expected result is that the amount of CS, Ag, and Zi used would be reduced as compared with normal amount while the antifungal ability still shows expected results. This study is anticipated to create a significant antimicrobial drug that is a safe fungicide for agriculture.

2 Materials and methods

2.1 Materials

Chitosan was purchased from Sigma Aldrich Co. (St. Louis, MO, USA) (CS, Mw 150,000, 75–85% deacetylated), acetic acid (CH_3COOH), silver nitrate (AgNO_3), and sodium hydroxide (NaOH) were purchased from Sigma-Aldrich (St. Louis, MO, USA). Zi Bul 80 WP was purchased

from Saigon Plant Protection Joint Stock Company (Ho Chi Minh City, Vietnam) (80% $\text{Zi C}_4\text{H}_6\text{N}_2\text{S}_4\text{Zn}$) was purchased from Saigon Plant Protection Joint Stock Company (Ho Chi Minh, Vietnam). All reagents and solvents were used without further purification.

2.2 Methods

2.2.1 Synthesis of the Ag@CS and Ag@CS-Zi: Ag@CS was synthesized by utilizing CS as a reducing and protecting polymer and AgNO_3 with NaOH by chemical reduction. Initially, CS (0.2 g, dissolved in 10 ml of 1% v/v CH_3COOH solution, pH 3.5) was mixed with AgNO_3 (2.5 ml, 1.0×10^{-2} M) under constant stirring for 30–45 min. After this step, the mixture of AgNO_3 and CS solution was obtained. Next, NaOH solution (10 ml, 1 M) was dropped into the mixture using a syringe pump. After 15–20 min, yellow-brown color spheres were washed to discard the residue, and Ag@CS was placed in the refrigerator to stop any further Ag reduction. Finally, Zi was combined with Ag@CS by soaking it in water at room temperature under constant stirring for 24 h. The volume ratio 2:1 between Zi and Ag@CS solution was used in the synergistic process.

2.2.2 Antifungal effect test of *Neoscytalidium dimidiatum*: To test the antifungal effect, the paper-disc method was used in this study. First, PDA agar plate (potato infusion at 200.00 g/l, dextrose 20.00 g/l, and agar 15.00 g/l) was prepared. Secondly, cell suspensions that contain fungi colonies were spread out directly on the agar surface. After that, round filter papers (diameter 5 mm) with dissolved AgNPs, CS, and compound Ag@CS were put in the plate. The inhibition zone diameter was measured. The differences between the controlled and treated samples were tested for significance using a t test ($p < 0.05$).

2.2.3 Characterization: The morphological characteristics of the synthesized nanoparticles were determined by TEM using FEI Tecnai G2 20 S-Twin at 100 kV. In order to characterize the thermal decomposition profiles of either CS or Ag@CS composites, TGA was performed on a TGA (Q500 V20.10 Build 36), and 5 mg specimens of both composites were measured with a nitrogen flow rate at a heating rate of $10^\circ\text{C}/\text{min}^{-1}$ from 30°C to 800°C . The FT-IR spectra were recorded with a Spectrum Tensor27 FT-IR Spectrometer, using KBr pellets FT-IR Spectrometer in the range of $500\text{--}4500\text{ cm}^{-1}$ with a resolution of 4 cm^{-1} . XRD patterns were obtained at room temperature using Cu K- α radiation ($\lambda = 1.5406\text{ \AA}$) with a range of $2\theta = 10^\circ\text{--}90^\circ$ and a scanning rate of 0.03 s^{-1} . The AgNPs were prepared by adding 20 μl CH_3COOH solution and 1 ml distilled H_2O to Ag@CS and then vortexed for 3–5 min. The Ag@CS was dropped to grid by a micropipette for further experiments.

3 Results and discussion

3.1 Characterization of nanoparticles

3.1.1 Particles size and morphology

The morphology and size of Ag@CS were provided by TEM (Figure 1). The particles were well separated and

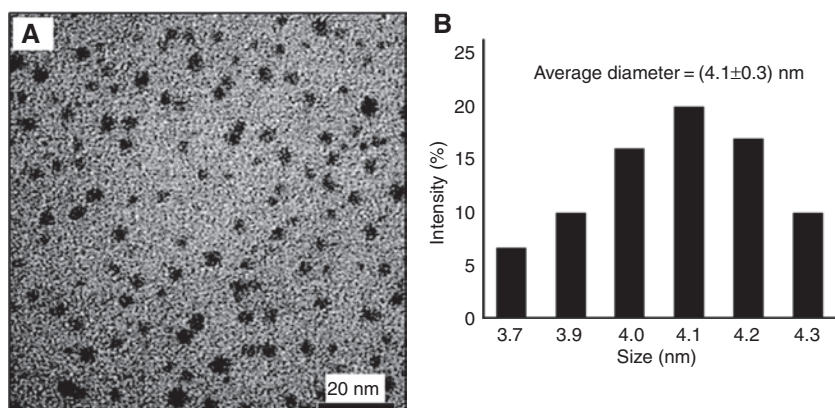


Figure 1: TEM image (A) and particle size distribution (B) of Ag@CS.

reasonably dispersed with a spherical shape and no more than 5 nm. The size of Ag@CS was measured to obtain an appropriate average diameter equal to 4.11 ± 0.37 nm, and this result was also consistent with XRD patterns. The size distributions of particles indicated that they were highly dispersed. The synthesized nanoparticles completely separated from each other without clumping, which increased the interactive efficiency between them and the drug and the surroundings. Compared with the shape of AgNPs and CS, Ag@CS had no significant differences in shape and size distribution, meaning that CS might act as a good stabilizing agent to prevent the aggregation of AgNPs and make them have a narrow size distribution in the crosslinking process [32, 39]. During the AgNPs synthesis, without any other chemical preservation, CS worked as scatter agents that eliminated the aggregation of particles. In 2011, M. Carmen Rodriguez investigated the average AgNPs below 2 nm [40]. This size was quite small for drug loading or combined with other components. The physico-chemical properties of nanoparticles are dependent on the size and properties of their surface. According to previous reports, nanoparticles range in size from 4 nm to 10 nm, which enables them to interact with their surroundings because of the enhanced permeability and retention effect. The mean particle size of the nearly spherical nanoparticles was 4 nm, which is the suitable size for the particles to be synergic and ensures their stability and specificity of their final purpose. Thus, the efficiency is increased significantly.

3.1.2 FT-IR analysis

The existence of chemical bond between CS and AgNPs was examined by FT-IR (Figure 2). The characteristic peaks of Ag@CS at 3421 cm^{-1} and CS at 3424 cm^{-1} are

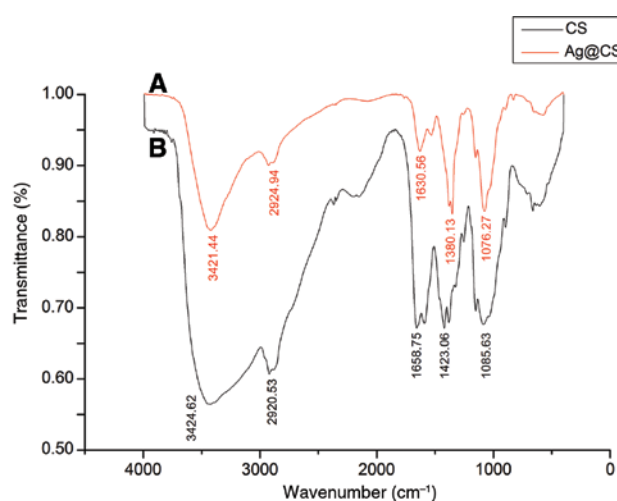


Figure 2: FT-IR spectra of Ag@CS (A) and CS (B).

consistent with the stretching vibrations of NH-amino in amino groups. The alkane C-H stretching lipids, specifically $-\text{CH}_2$ and $-\text{CH}_3$ groups of CS and Ag@CS, are shown in the bands between 2920 cm^{-1} and 2924 cm^{-1} . The bands of CS at 1658 cm^{-1} and of Ag@CS at 1630 cm^{-1} are related to the amino groups of amide. The C=C peak of aromatic amine groups is associated with 1380 cm^{-1} peak. The bands between 1076 cm^{-1} and 1085 cm^{-1} are assigned the protein stretch carbonyl that is present in CS. It can be seen that through free amine groups, protein-bound AgNPs is a stabilizing agent which reduces AgNO_3 to form AgNPs during the process. Besides, the AgNPs peak at 1492 cm^{-1} and $-\text{NH}_2$ stretch at 1423 cm^{-1} of CS shift to 1380 cm^{-1} in nanoparticles composite curve. It illustrates that $-\text{NH}_2$ or $-\text{OH}$ groups of CS are combined with Ag^+/Ag^0 via electrostatic bond. This result was also affirmed by Vigneshwaran's research [41]. Moreover, the band of O-H group at 3421 cm^{-1} and stretch of primary amine at 1659 cm^{-1} are not shown,

which demonstrated the attachment of Ag to nitrogen atom. These results indicate the presence of electrostatic bond between CS and Ag, creating a composite Ag@CS.

3.1.3 X-ray diffraction analysis

Figure 3 illustrates the XRD patterns of Ag@CS. The broad reflection at 9° is due to the crystallinity of CS in composites. Besides, the Bragg reflections at 38.16° , 46.12° , 64.09° , 77.01° , and 86° are assigned to diffractions from the (2.336), (1.947), (1.380), (1.237), and (1.129) indexed planes of metallic Ag nanoparticles. The pattern of AgNPs and pure CS result shows the unchanged crystalline structure of AgNPs after being introduced into CS polymer.

3.1.4 Thermogravimetric analysis

In order to analyze the thermal stability of Ag@CS and CS, TGA is shown in Figure 4. In the $50\text{--}800^\circ\text{C}$ range, the samples show two distinct weight loss stages: (1) From 50 to 150°C , 10% weight was lost because of water evaporation in Ag@CS sample ($50\text{--}100^\circ\text{C}$), whereas CS, which was dried up, still decreased its weight at a temperature higher than 100°C (lower than normal decomposition of CS). This is because the original CS exists not only the long chain of polymers but also many short oligomer CS that leads to short-term thermal stability; (2) from 150 to 800°C , thermal decomposition of Ag@CS complexes was lower than that of CS. This result indicates that when AgNPs is embedded in CS polymer, Ag can break down the structure

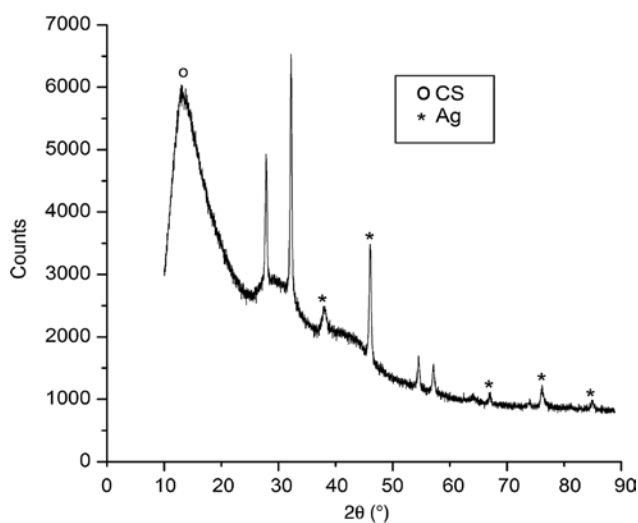


Figure 3: XRD pattern of Ag@CS.

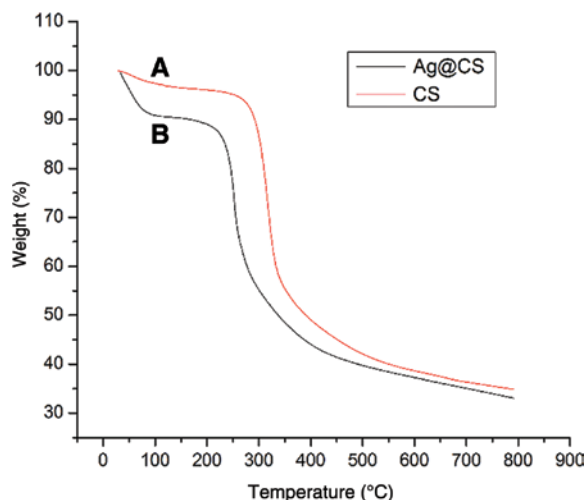


Figure 4: Thermogravimetric curves of CS (A) and Ag@CS (B).

of CS during the process of dissolving in acid and base; therefore, the reduction in weight of CS synergized with Ag was higher than original CS.

3.2 Antifungal activity test

The antifungal activity of Ag, Zi, Ag@CS, and Ag@CS-Zi was estimated against *N. dimidiatum* by agar diffusion method. A blank control plate was of pure cell suspension without any other components. In comparison with an effective antifungal ability, four different concentrations of Ag, Zi, Ag@CS, and Ag@CS-Zi were used as comparative samples (Table 1).

According to the table, the antifungal ability was quite low when using AgNPs alone. However, when Ag was combined with CS, fungicidal capability was increased significantly (Figure 5). The diameter of the zone of inhibition was 15.00 ± 0.00 mm at 5 ppm which was completely better than the diameter with concentration at 10 ppm (13.33 ± 0.58 mm). When Zi was combined with Ag@CS, the antifungal ability was increased considerably. While pure Zi at 500 ppm and 1000 ppm was incapable of eliminating the fungi, the inhibited zone of Ag@CS-Zi increased to 12.00 ± 0.00 mm, nearly equal to the diameter when using 5 ppm Ag (12.33 ± 0.58 mm) and much higher when using 5000 ppm of Zi (9.00 ± 0.00 mm). The diameter of inhibition zone of Ag@CS-Zi at 2500 ppm of Zi was 20.67 ± 0.58 , which showed its high antifungal activity compared with each individual component. In particular, the synergistic effect of Ag@CS at 2 ppm and Zi at 5000 ppm indicated high and strong antimycotic ability. After a series of experiments, it can be concluded that the concentration of Ag@

Table 1: The diameters of inhibited zone of Ag, Ag@CS, and Ag@CS-Zi.

Concentration (ppm)			Average inhibition zone diameter (mm)
Ag	CS	Zi	
1	—	—	07.67 ± 0.58
2	—	—	10.50 ± 0.50
5	—	—	12.33 ± 0.58
10	—	—	13.33 ± 0.58
1	2000	—	07.80 ± 0.20
2	4000	—	11.67 ± 0.58
5	10,000	—	15.00 ± 0.00
10	20,000	—	17.42 ± 0.52
—	—	500	05.00 ± 0.00
—	—	1000	05.00 ± 0.00
—	—	2500	07.83 ± 0.29
—	—	5000	09.00 ± 0.00
2	4000	500	12.00 ± 0.00
2	4000	1000	15.33 ± 1.53
2	4000	2500	20.67 ± 0.58
2	4000	5000	25.33 ± 0.58

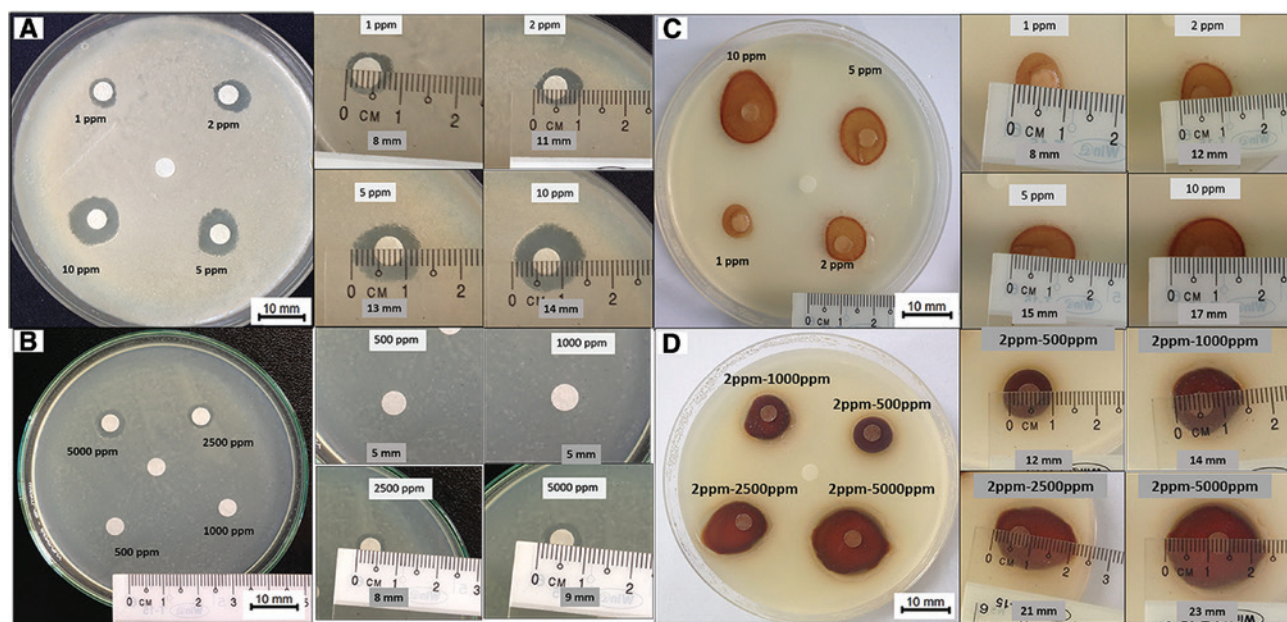
CS at 2 ppm provided the optimal antifungal conditions in combination with different concentrations of Zi in this study.

Due to synergy between Ag@CS and Zi, the required concentration for each component decreased remarkably while the result was extremely good. With the nearly 2.5 times decreased concentration in 400–600 l of mixture/ha, these concentrations of Ag are completely safe for the users, plants, and the environment. Farmers'

health could be totally protected. Moreover, the amount of Ag expelled to the environment is not enough to cause environmental pollution or any dangerous chemical problems for fungal activity in particular and for antimicrobial applications in general. Ag@CS exhibited antifungal properties with low concentration of both AgNPs and CS participating in the compound. The Ag@CS should be expected to behave as a biomaterial to be used in different agriculture applications, mainly in antimicrobial treatments.

4 Conclusion

In this study, AgNPs were combined with functionalized CS, which improved the stability and synergized with the fungicide to enhance antifungal activity. According to the results of FT-IR and XRD analysis, fungicide-loaded Ag@CS were successfully synthesized. TEM imaging showed that the Ag@CS was nearly spherical in shape with diameter of 4.11 ± 0.37 nm. The study demonstrated that Ag@CS had good result in killing fungi. The antifungal ability of Ag enhanced the fungicidal effect of CS. Basing on Ag@CS, the new approaches for many kinds of antifungal, antibacterial, antiviral, and other substances might be developed and improved. It is considered as an important step for antimicrobials in agriculture to contribute to reduction of amount of pesticides and elimination of harmful products. In short, the reduced amount of pesticide not only

**Figure 5:** Average inhibition zones observed of AgNPs (A), Zi (B), Ag@CS (C), and Ag@CS-Zi (D) against *Neoscytalidium dimidiatum*.

protects human health but also improves the fruit quality and protects the environment.

Acknowledgements: This work was financially supported by a grant from the Viet Nam Academy of Science and Technology, Institute of Applied Materials Science, Ho Chi Minh.

References

- [1] Chau D. Manufacturing and sustainable development of dragon market. <http://www.mard.gov.vn/2014>.
- [2] Ariffin AA, Bakar J, Tan CP, Rahman RA, Karim R, Loi CC. *Food Chem.* 2009, 114, 561–564.
- [3] Selvig T, Porter P. Biologic-chemical fungicide compositions and methods of use. Google Patents; 2002.
- [4] Zee F, Yen C-R, Nishina M. Hawaii Univ. 2004, 3.
- [5] Masyahit M, Sijam K, Awang Y, Ghazali M. *Int. J. Agric. Biol.* 2009, 11, 659–666.
- [6] Marcoux C, Urpelainen J. *Rev. Policy Res.* 2011, 28, 585–612.
- [7] Wichienchot S, Jatupornpipat M, Rastall R. *Food Chem.* 2010, 120, 850–857.
- [8] Zheng L-Y, Zhu J-F. *Carbohydr. Polym.* 2003, 54, 527–530.
- [9] Vakis RM, Williams R. *J. Hortic. Sci.* 1978, 53, 91–94.
- [10] Belden J, McMurry S, Smith L, Reilley P. *Environ. Toxicol. Chem.* 2010, 29, 2477–2480.
- [11] Meco G, Bonifati V, Vanacore N, Fabrizio E. *Scand. J. Work Env. Hea.* 1994, 20, 301–305.
- [12] Woo K, Ngou F, Ngo L, Soong W, Tang P. *Am. J. Food Technol.* 2011, 6, 140–148.
- [13] To LV, Ngu N, Duc ND, Trinh DT, Thanh NC, Mien DV, Hai CN, Long TN. *The Australian Centre for International Agricultural Research Proceedings* 1999, 100.
- [14] Seltenrich N. *Environ. Health Persp.* 2013, 121, a220.
- [15] Echegoyen Y, NerĀn C. *Food Chem. Toxicol.* 2013, 62, 16–22.
- [16] Monteiro DR, Gorup LF, Takamiya AS, Ruvollo-Filho AC, de Camargo ER, Barbosa DB. *Int. J. Antimicrob. Ag.* 2009, 34, 103–110.
- [17] Kumar R, MĀĥnstedt H. *Biomaterials* 2005, 26, 2081–2088.
- [18] Ishihara M, Nguyen VQ, Mori Y, Nakamura S, Hattori H. *Int. J. Mol. Sci.* 2015, 16, 13973–13988.
- [19] Jo Y-K, Kim BH, Jung G. *Plant Dis.* 2009, 93, 1037–1043.
- [20] PanĀček A, Kvĥtek L, Pucek R, Kolar M, Vecerova R, Pizurova N, Sharma VK, NeveĥnĀ Tj, Zboril R. *J. Phys. Chem. B* 2006, 110, 16248–16253.
- [21] Kokura S, Handa O, Takagi T, Ishikawa T, Naito Y, Yoshikawa T. *Nanomed. Nanotechnol. Biol. Med.* 2010, 6, 570–574.
- [22] Cho K-H, Park J-E, Osaka T, Park S-G. *Electrochim. Acta* 2005, 51, 956–960.
- [23] Sotiriou GA, Pratsinis SE. *Environ. Sci. Technol.* 2010, 44, 5649–5654.
- [24] Holladay RJ, Moeller W, Mehta D, Roy R, Brooks JH, Mortenson MG. Silver/water, silver gels and silver-based compositions; and methods for making and using the same. Google Patents; 2005.
- [25] Twu Y-K, Chen Y-W, Shih C-M. *Powder Technol.* 2008, 185, 251–257.
- [26] Pang X, Zhitomirsky I. *Surf. Coat. Tech.* 2008, 202, 3815–3821.
- [27] Marin E, Briceĥo MI, Caballero-George C. *Int. J. Nanomed.* 2013, 8, 3071.
- [28] Ramezani Z, Zarei M, Raminnejad N. *Food Control* 2015, 51, 43–48.
- [29] Archana D, Singh BK, Dutta J, Dutta P. *Int. J. Biol. Macromol.* 2015, 73, 49–57.
- [30] Kumar-Krishnan S, Prokhorov E, HernĀĥdez-Iturriaga M, Mota-Morales JD, VĀĥquez-Lepe M, Kovalenko Y, Sanchez IC, Luna-BĀĥrcenas G. *Eur. Polym. J.* 2015, 67, 242–251.
- [31] Lĥpez-Carballo G, Higuera L, Gavara R, HernĀĥdez-Muĥoz P. *J. Agr. Food Chem.* 2012, 61, 260–267.
- [32] Yadollahi M, Farhoudian S, Namazi H. *Int. J. Biol. Macromol.* 2015, 79, 37–43.
- [33] Mishra SK, Ferreira J, Kannan S. *Carbohydr. Polym.* 2015, 121, 37–48.
- [34] Cao X, Cheng C, Ma Y, Zhao C. *J. Mater. Sci. Mater. Med.* 2010, 21, 2861–2868.
- [35] Wei D, Sun W, Qian W, Ye Y, Ma X. *Carbohydr. Res.* 2009, 344, 2375–2382.
- [36] Sacco P, Travan A, Borgogna M, Paoletti S, Marsich E. *J. Mater. Sci. Mater. Med.* 2015, 26, 1–12.
- [37] Luan LQ, Ha VT, Nagasawa N, Kume T, Yoshii F, Nakanishi TM. *Biotechnol. Appl. Biochem.* 2005, 41, 49–57.
- [38] Huang H, Yuan Q, Yang X. *Colloid. Surface. B* 2004, 39, 31–37.
- [39] An J, Yuan X, Luo Q, Wang D. *Polym. Int.* 2010, 59, 62–70.
- [40] Rodrĥguez-Argĥelles MC, Sieiro C, Cao R, Nasi L. *J. Colloid Interf. Sci.* 2011, 364, 80–84.
- [41] Vigneshwaran N, Ashtaputre N, Varadarajan P, Nachane R, Paralikar K, Balasubramanya R. *Mater. Lett.* 2007, 61, 1413–1418.

Bionotes



Uyen Thi Phan Ngoc

Uyen Thi Phan Ngoc obtained her Bachelor of Biotechnology from Ho Chi Minh City International University, Vietnam, in August 2016. She now works as a research assistant with Dr. Dai Hai Nguyen at the Institute of Applied Materials Science, Vietnam Academy of Science and Technology. Her major research is related to synthesis and characterization of nanomaterials as a drug delivery system for cancer therapy.



Dai Hai Nguyen

Dai Hai Nguyen obtained his PhD from Ajou University, Republic of Korea, in 2013. Currently, he works as a researcher at the Institute of Applied Materials Science, Vietnam Academy of Science and Technology. He is also an invited lecturer at Tra Vinh University and Ho Chi Minh City University of Natural Sciences.